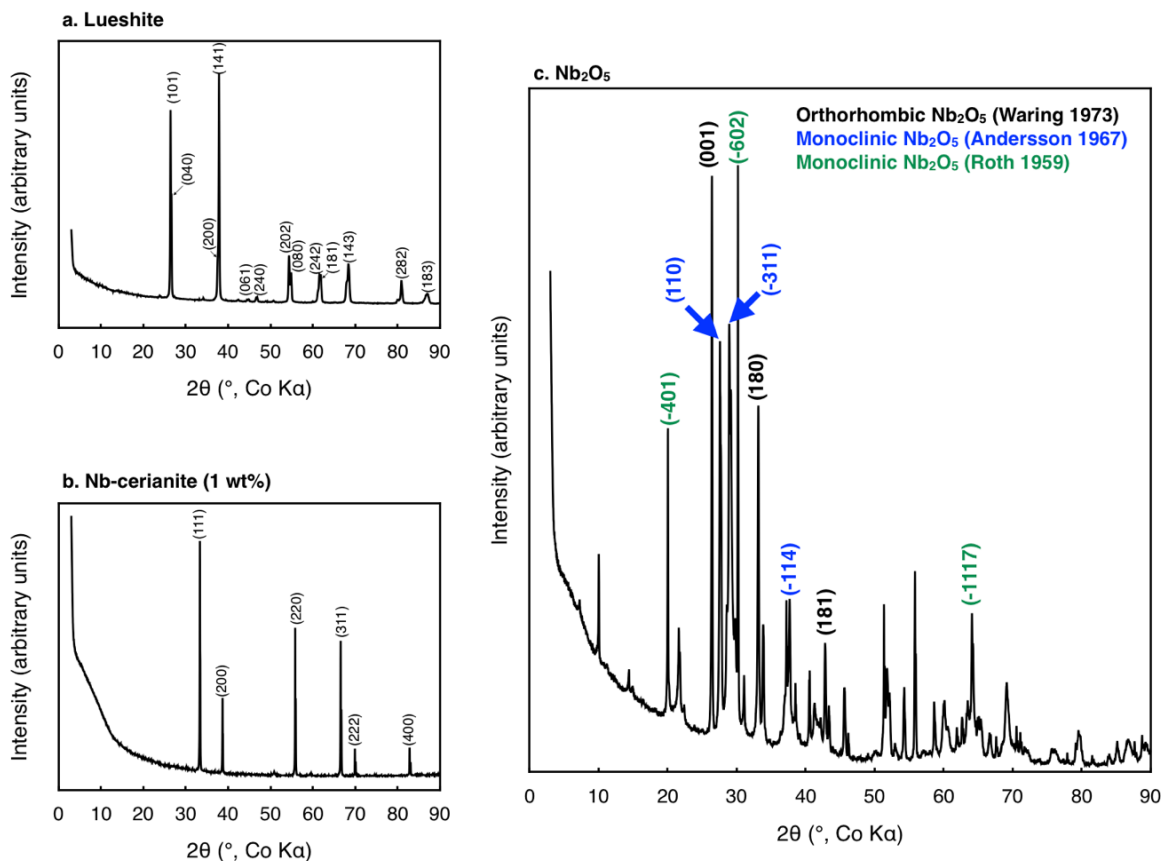
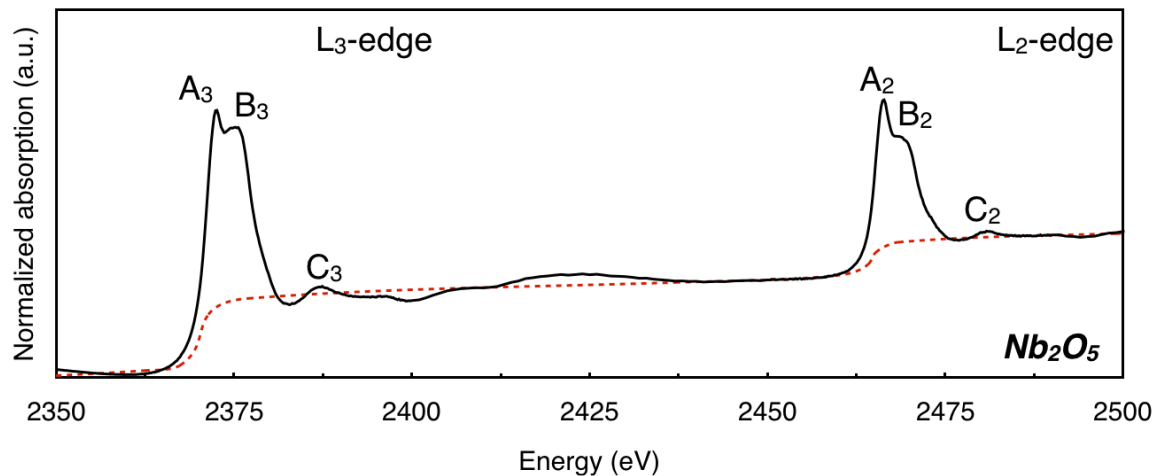


**FIGURE S1.** X-ray diffraction patterns with annotated Miller indices of (a) Nb-substituted Fe oxides, (b) Nb-substituted Ti oxides.



**FIGURE S2.** X-ray diffraction patterns with annotated Miller indices of the other synthetic references (a) lueshite, (b) Nb-substituted cerianite, and (c) Nb<sub>2</sub>O<sub>5</sub>.



**FIGURE S3.** MBACK normalization method of  $\text{Nb}_2\text{O}_5$  Nb  $L_{2,3}$ -edges XANES spectrum (black line). The MBACK normalization curve (dashed red line) is dominated by a Legendre polynomial term with an additional error function term (Weng et al. 2005). The edge energy chosen as the input parameter of the MBACK function implemented in Larch is ca. 2371 eV.

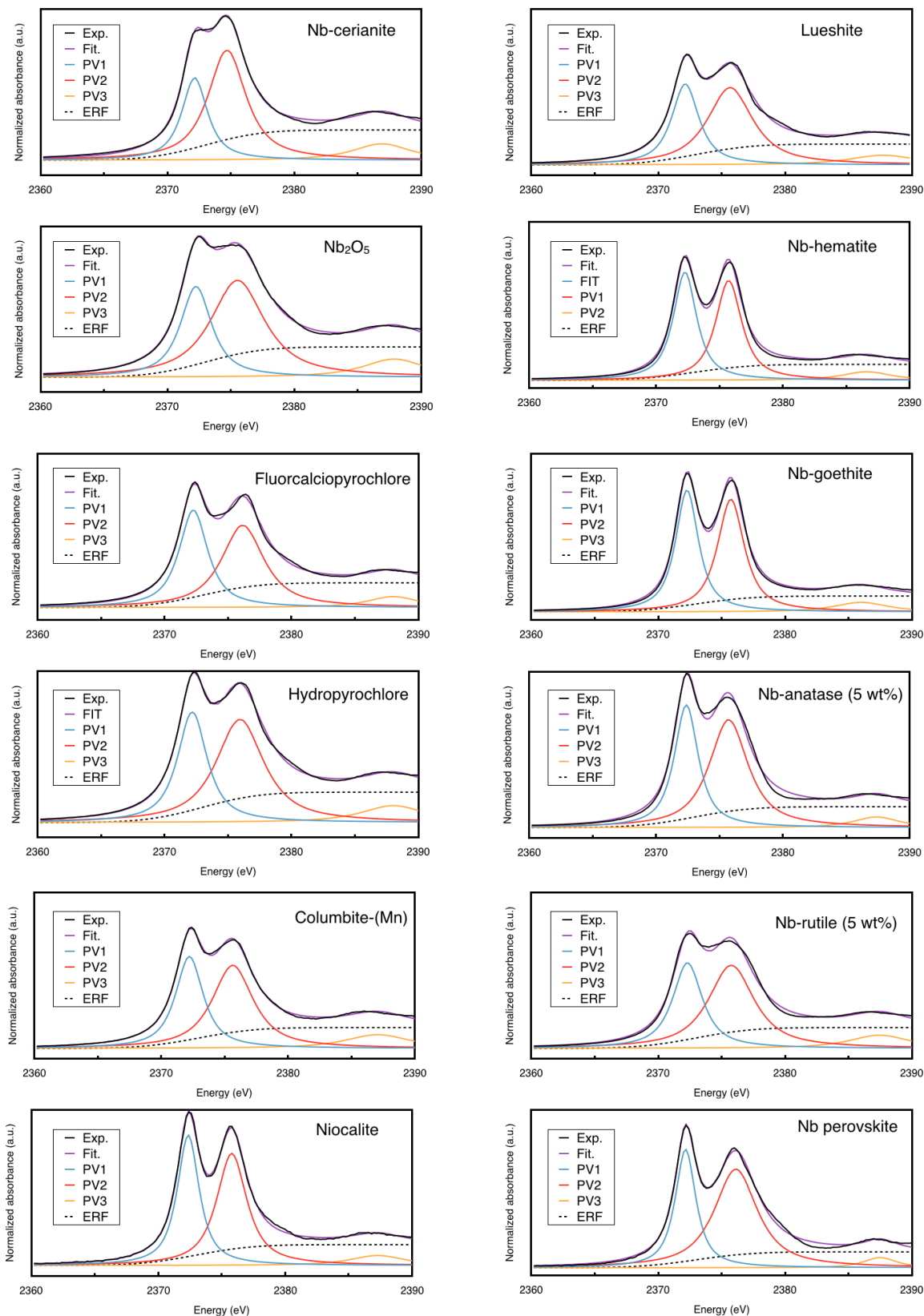


**FIGURE S4.** Deconvolution of the  $L_3$ -edge for the complete set of reference spectra with three pseudo-Voigts (PV1, PV2, PV3) and a step error function (ERF). The experimental (Exp.) and the fitted data (Fit.) are shown by the black and purple curves, respectively.

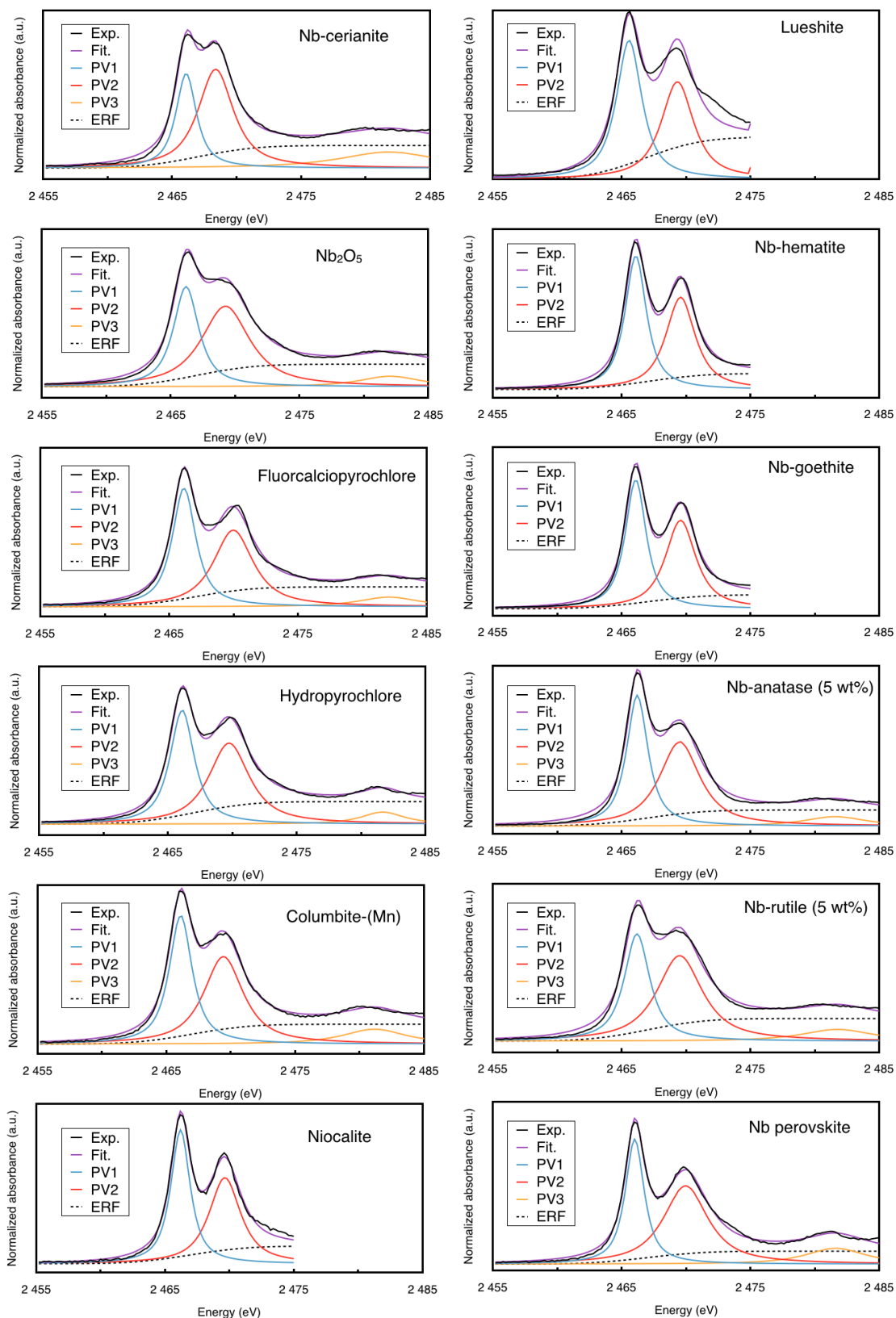


**FIGURE S5.** Deconvolution of the  $L_2$ -edge for the complete set of reference spectra with three pseudo-Voigts (PV1, PV2, PV3) and a step error function (ERF). The experimental (Exp.) and the fitted data (Fit.) are shown by the black and purple curves, respectively.

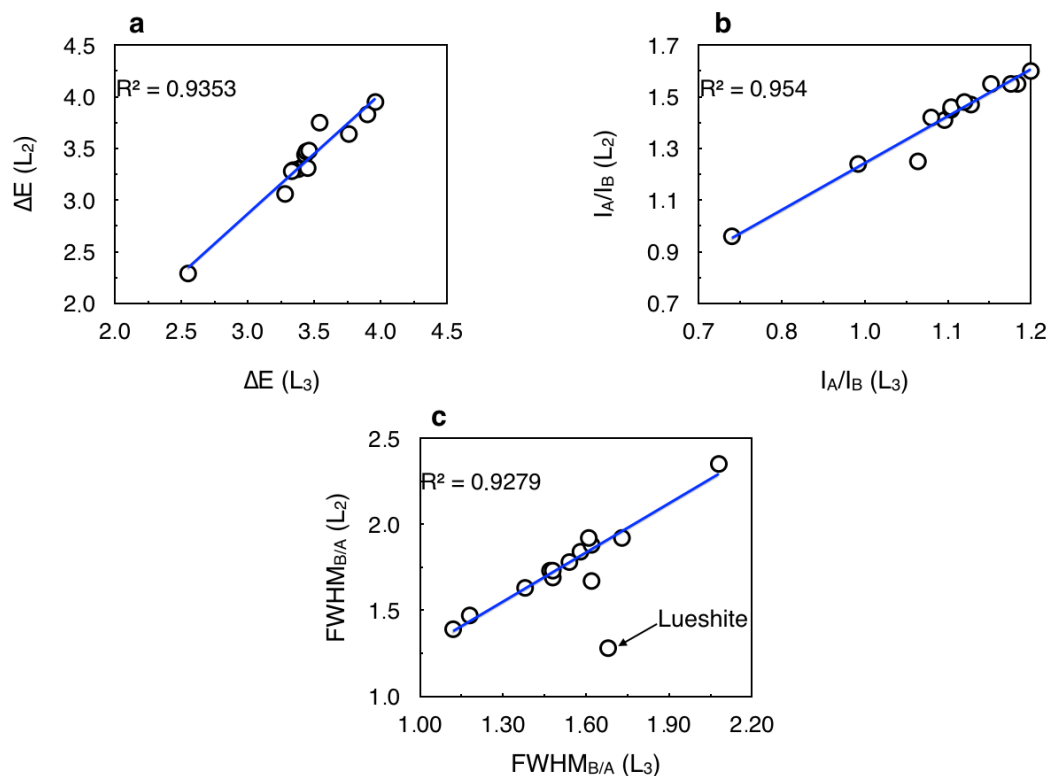


**FIGURE S6.** Binary plots of the correlation of (a)  $\Delta E$ , (b)  $I_A/I_B$ , and (c)  $FWHM_{B/A}$  between the  $L_3$ - and the  $L_2$ -edges. Pearson's correlation coefficients are given after excluding lueshite data.

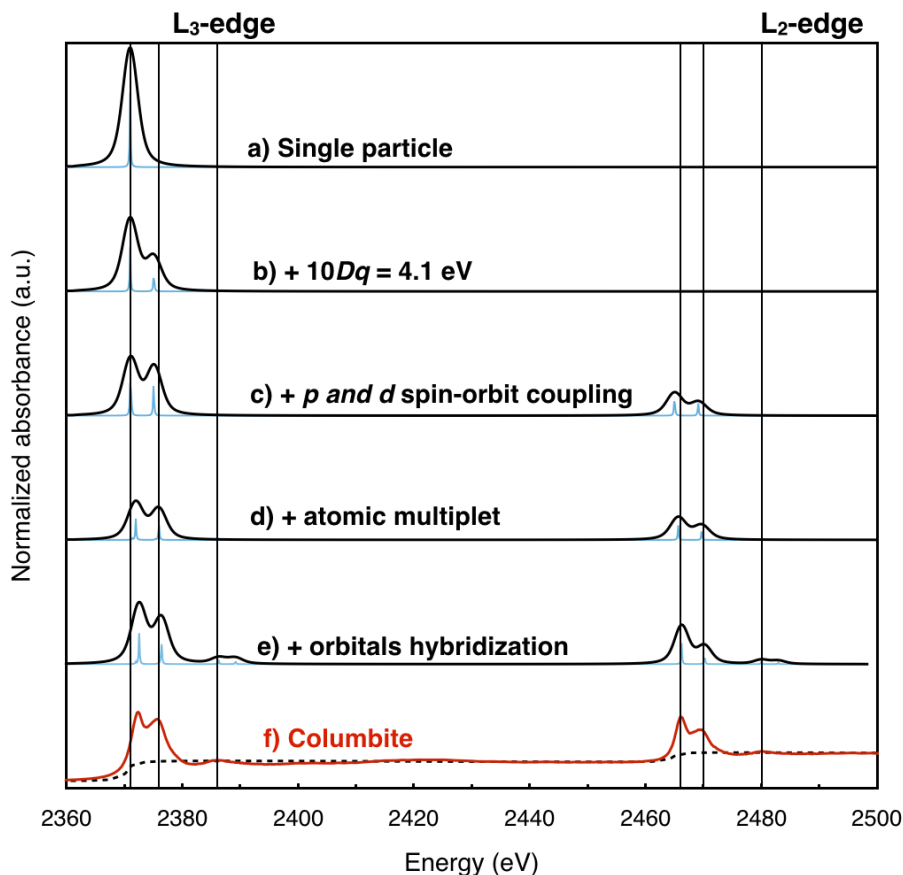


**FIGURE S7.** Theoretical spectra reproduce experimental spectra (such as the one of columbite here) when crystal-field and ligand-field multiplet effects are taken into account in the simulations. **(a)** Atomic spectrum for the  $2p^64d^0 \rightarrow 2p^54d^1$  transition of  $\text{Nb}^{5+}$  ions. **(b)** Addition of crystal-field effects with Nb occupying a regular octahedral site ( $O_h$ ).  $10Dq = 4.1$  eV was chosen in order to simulate the columbite spectrum. **(c)** Inclusion of  $2p$  (scale factor of 0.98) and  $4d$  spin-orbit coupling. **(d)** Inclusion of atomic multiplet effects with Slater-Condon integrals scaled to 80% of their atomic values ( $F^2pd = 1.972$  eV,  $G^1pd = 1.627$  eV and  $G^3pd = 0.946$  eV). **(e)** Inclusion of ligand-field multiplet effects involving the hybridization of the  $2p$  (O) and  $4d$  (Nb) orbitals. **(f)** Experimental spectrum of columbite. Experimental spectra must be normalized (MBACK curve, dashed line) and absorption background must be removed to be compared with theoretical spectra.

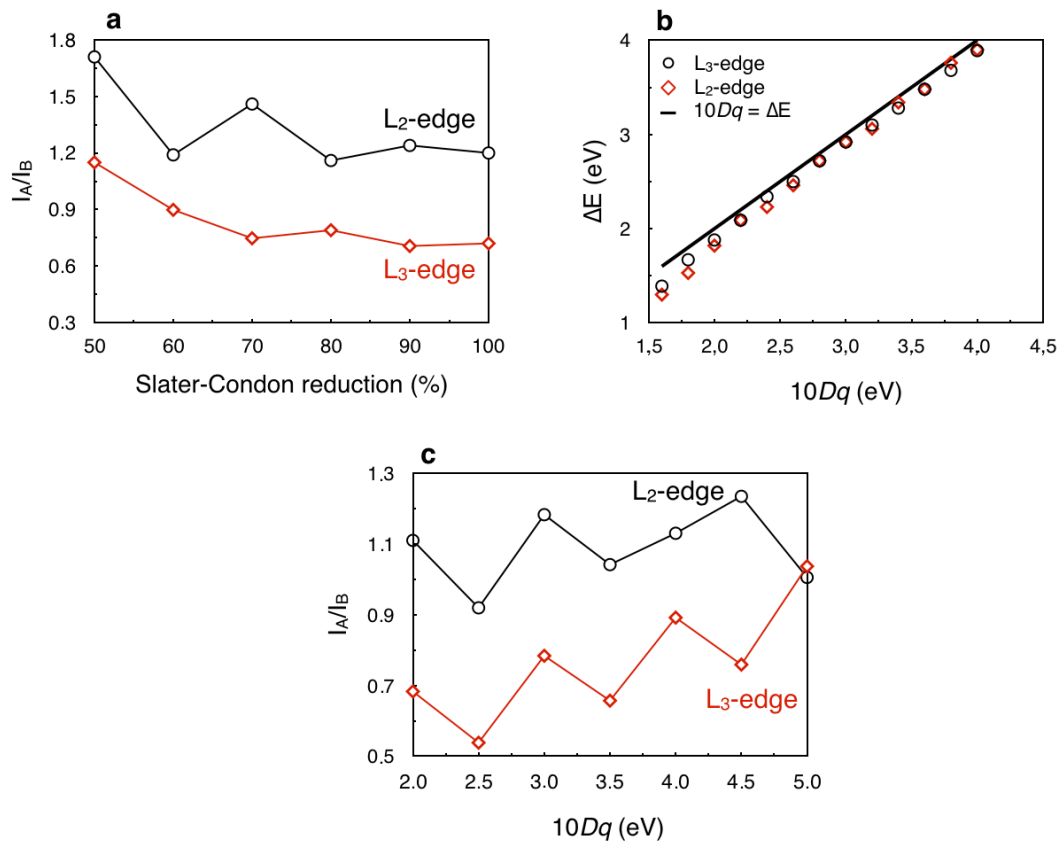
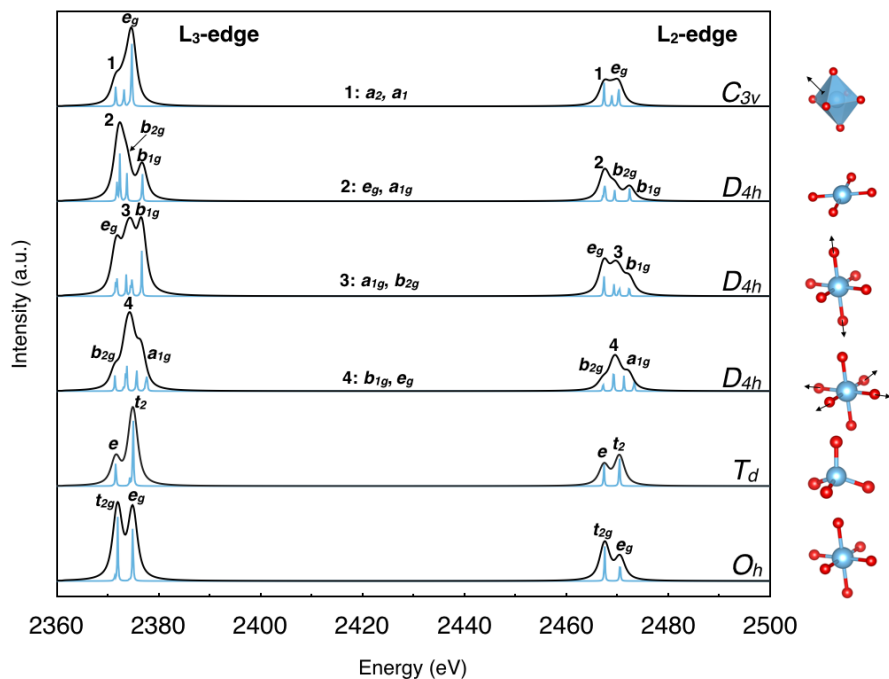


FIGURE S8. Binary plots of (a) the correlation between  $10Dq$  and  $\Delta E$ , (b) and c)  $I_A/I_B$  ratio with respect to  $10Dq$  and Slater-Condon reduction factor.





**FIGURE S9.** Influence of the local symmetry of Nb site on the spectral Nb  $L_{2,3}$ -edges XANES features. (a)  $O_h$  symmetry (regular  $^{60}\text{Nb}$  octahedron). (b)  $T_d$  symmetry ( $^{14}\text{Nb}$ ). (c)  $D_{4h}$  symmetry (compressed  $^{60}\text{Nb}$  octahedron). (d)  $D_{4h}$  symmetry (elongated  $^{60}\text{Nb}$  octahedron). (e)  $D_{4h}$  symmetry ( $^{14}\text{-sq}$  Nb square plane). (f)  $C_{3v}$  symmetry (trigonal distortion of the  $^{60}\text{Nb}$  octahedron).